B meson Measurements using HFT

1. Introduction

The bottom and charm quark are expected to behavior very differently in the QGP due to their large difference in mass[1]. The surprising observation of large suppression of high p_T non-photonic electron production has triggered a lot of developments on models involving dramatically different bottom charm meson production mechanism.[2,3,4,5,6,7.] Similarly, large non-photonic electron elliptic flow is observed in the low p_T region but there is the tendency of flow reduction at higher p_T possibly due to bottom quark contribution. Independent measurements on bottom quark production would be critical to disentangling different heavy meson production mechanisms and provide crucial information on the medium properties. On the other hand, measurement of bottom meson is important to clarifying the J/ψ production mechanism in the medium. Apart from the primordial production, a significant fraction of J/ψ comes from the B meson decay. Measurements on B meson production would allow us to subtract the contamination from B-decay component.

With current detector configuration, the estimation of B contribution to the non-photonic electron spectrum was estimated to be ~50% at pT>5 GeV/c[8] with large uncertainties. With HFT, the measurements are expected to be dramatically improved. Besides exclusive measurements with large luminosity, B mesons are usually measured using leptons and J/ψs through their semi-leptonic decay and J/ψ decay channels, respectively.

2. Measurement Methods

When measuring B meson using leptons from their semi-leptonic decay, we utilized the impact parameter (d_0) method used by the ALICE collaboration[9] to separate electrons of B decays from those of D decays. Since B mesons have mean proper decay lengths of ~500 μm, their decay electrons are characterized by large impact parameters with respect to the interaction vertex. With the two pixel layers which instrument the innermost part of the HFT, the tracks' d_0 will be measured in STAR with a resolution $\sigma_{d0} \sim 20$ μm for $p_T \geq 2$ GeV/c. A cut imposing a minimum value of d_0 rejects a large fraction of the electrons from light meson decays and photon conversions, as well as primary pions misidentified as electrons. The charm contamination will be reduced with a p_T cut, as electrons of B decays have a harder p_T distribution than those of D decays due to the larger mass of the b quark. The UA1 Collaboration[10] has developed a Monte-Carlo method to extract the minimum- p_T -differential cross section at the B-meson level from the decay-electron p_T differential cross section, assuming the B-meson decay kinematics is well understood.

When measuring B meson through their decay J/ψs, we utilized the method developed by CDF[11] to calculate the pseudo-cτ of J/ψ and apply a certain cut on it to distinguish direct and B-decay J/ψ. Figure 1 illustrates how different variables are defined. The pseudo-cτ is defined as $c\tau' = \vec{L} \cdot \frac{p_T^{\psi}}{\left|p_T^{\psi}\right|} \cdot \frac{M_{\psi}}{\left|p_T^{\psi}\right|}$, where $\vec{L}$ is the path length between the J/ψ production

point and collision vertex, M_ψ is the J/ψ mass and p_T^ψ is the J/ψ p_T which is required to be larger than 1.25GeV/c. Additionally, we define DCA as the distance of closest approach between paired electrons. A DCA cut of 50 μm is applied since the simulation shows the DCA for electron pairs from J/ψ are mostly within this range. The pseudo-cτ is less than 15% smaller[12] than the actual B meson cτ. In this analysis, the only physical background considered here is direct J/ψ including feed-down contribution from higher mass charmonium states. Charm continuum and Drell/Yan might have similar level of contribution (see later discussions). The background due to the random combination of electron pairs during the mass reconstruction is removed via subtracting the same sign electron pair when analyzing mass and pseudo-cτ distribution. The signals are $B^{\pm}/B^0$ mixture which has a 1.094% branching ratio to decay to J/ψ[13].

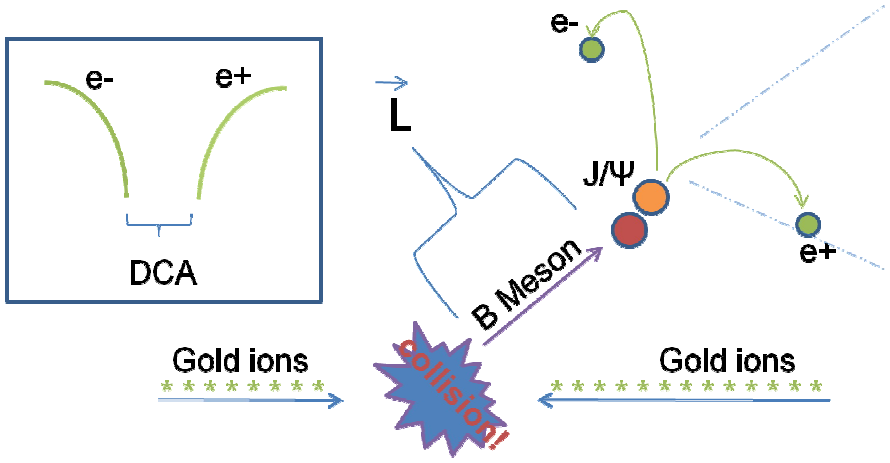

Figure 1: definition of variables used in the analysis. See text for details.

3. Simulation procedure

In the simulation for B meson semi-leptonic decay, we used the geometry described in HFT CD0 proposal[14]. We first generated 3600 HIJING background events for central (b < 3 fm) Au+Au collisions at 200 GeV, with vertex Z between -5 and 5 cm for the best utilization of the pixel layers. Then for each event, we embedded 10 B^+ mesons which were forced to decay only into neutrino, positron and $\overline{D^0}$, and 10 D^+ mesons which were forced to decay only into neutrino, positron and $\overline{K^0}$. The B and D mesons were required to have a flat p_T distribution to enhance the statistics at high p_T , and p_T weights were applied later in the analysis to mimic the spectra in reality. The embedded events then went through the STAR data reconstruction chain to simulate the particle tracking by STAR detectors, and were stored into the standard data files for analysis.

In the simulation for B→J/ψ decay, we use the same geometry. PYTHIA is used to generate 353.5k direct J/ψ→e+e- and 162.1k B→J/ψ→e+e- decay in full phase space. Comparison of the acceptance of J/ψ with collision Z vertex at the center of STAR and within ±5cm shows little difference, we therefore fixed the collision vertex at the STAR center in most of the simulation for simplicity. These J/ψs are then embedded into most

central Au+Au collisions generated from HIJING. Every 20 J/ψs are embedded into one single HIJING events to save computing time. Finally all the events are pushed through STAR reconstruction chain to simulate realistic detector response. We also reconstructed a similar amount of direct and B-decay J/ψ in most central Au+Au collisions including PIXEL detector pile-up effect from 1× RHIC-II luminosity.

4. Results and discussion.

4.1. Measurements through B semi-leptonic decay,

In the analysis, we applied the p_T weights so that B/D spectrum and their relative contributions to non-photonic electrons follow the FONLL calculations[15], and the combined electron sample from B^+ and D^+ decays obeys the measured non-photonic electron spectrum for central (0-5%) Au+Au collisions at 200 GeV[16]. As a result, the simulation input of the non-photonic electron p_T yields is shown in the left panel of Figure 2, normalized by the number of minimum bias events with vertex Z between -5 and 5 cm. The total tracking efficiency is ~55%, including both the TPC and the HFT pixel layers. Figure 3 presents the simulation results of the impact parameter distributions of electrons from B and D decays, for four p_T bins. Similar with the estimations in Ref.[8], the non-photonic electron sample is dominated by the D contribution for $2 < p_T < 3$ GeV/c, and the B contribution increases with p_T.

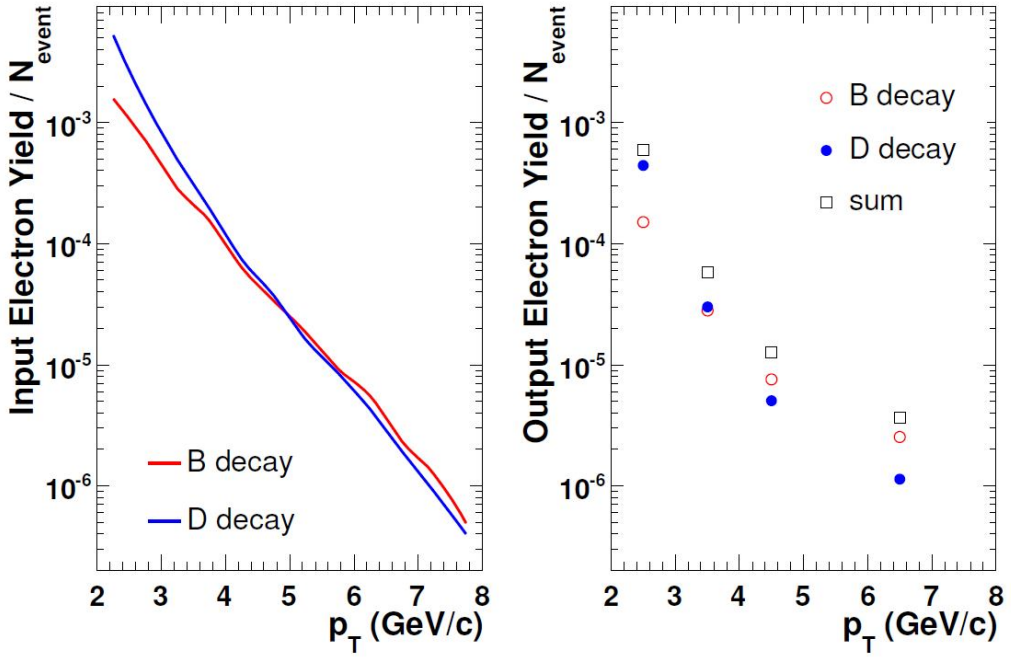

Figure 2: The simulation input (left panel) and output (right panel) of the non-photonic electron yields as a function of p_T , normalized by the number of minimum bias events with vertex Z between -5 and 5 cm.

Above 4 GeV/c, there is a d_0 region (200−600 μm) where the B contribution is dominant. We selected electrons within this d_0 region to enhance the B contribution, and the electrons satisfying this condition were counted for each p_T bin, and the output is plotted in the right panel of Figure 2. The purities of the B-tagged electrons are 25%, 48%, 60% and 69% respectively, from low to high p_T bins, and the yields are 150, 28, 7.5 and 2.5

per million minimum bias central Au+Au events with vertex Z between -5 and 5 cm. The ALICE Coll. reported the purity of B-tagged electrons to be 80% for the collisions at LHC with the same method[17]. When we tried our approach with the FONLL B contribution [15] for LHC, we did see a purity of ~80% for p_T > 4 GeV/c. The purity obtained in this approach depends on the relative B/D contribution, which is an input yet to measure. In the analysis of the real data, we first go through the above simulation procedures without applying the weight for the relative B/D contribution, and leave the simulated d_0 distributions un-normalized for electrons from B and D separately for each p_T bin. The measured d_0 distribution will then be fit with a parameterized combination of the simulated d_0 distributions for electrons from B and D, and the relative B/D contribution will be retrieved as fitting parameters. With the relative B/D contribution measured, we can estimate the purity of B-tagged electrons for different DCA regions, and determine the optimal cuts for B reconstruction.

We have estimated the feasibility of the impact parameter method for the proposed STAR HFT detector with the worst case: all the D-decay electrons come from D^+ mesons, whose

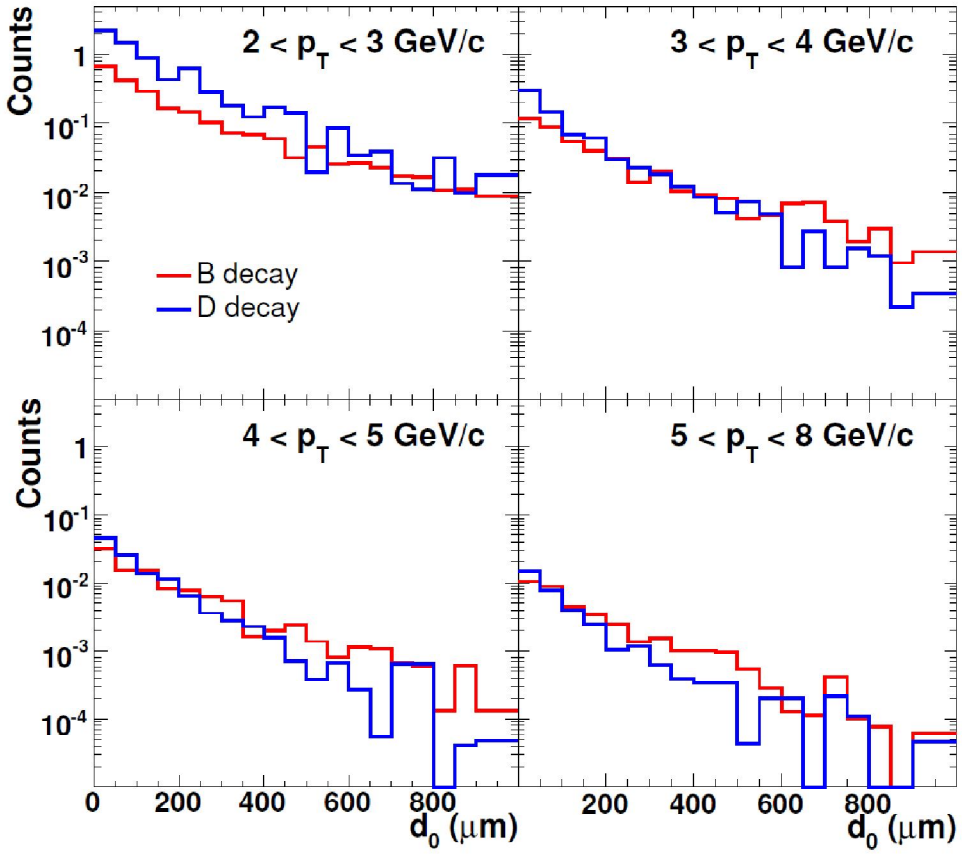

Figure 3: The simulation results of the impact parameter distributions of electrons from B and D decays.

decay length is ~300 μm. In reality, D^0 and D_s^0 mesons also decay into a substantial portion of D-decay electrons, and the corresponding decay length is only ~100 μm. In future, we will consider the more realistic case, where the D-decay electrons in the d_0

region (200−600 μm) should be significantly suppressed, and hence, the purity of B-tagged electrons should increase. The yield of B-tagged electrons above 4 GeV/c is 10 per million minimum bias central Au+Au events with vertex Z between -5 and 5 cm. This number was obtained with the assumption of a 100% efficiency of the electron identification, which could be only 10% in reality, depending on the detectors involved and the identification approach. However, we can enhance the statistics of high-p_T electrons by applying high-tower triggers using STAR BEMC. When triggering on the track's minimum energy deposition in the BEMC tower, we can almost guarantee one high-p_T electron per event. The electron yield above 4 GeV/c could be enhanced by 5000 times. All the discussions above are focusing on the Au+Au collisions. We will also carry out the simulations for p+p collisions.

4.2. Measurements through B→J/psi+X decay

The goal of this analysis is to obtain the S/B ratio and efficiency as a function of pseudo-$c\tau$ cut in most central Au+Au collisions with and without the addition of PIXEL detector pile-up effect in RHIC-II luminosity.

In the analysis, the J/ψ signal is obtained by subtracting like-sign electron pairs mass spectrum from the unlike-sign electron pair spectrum within a mass window between 2.8GeV/c^2 and 3.2GeV/c^2. Figure 4 shows the mass distribution for unlike-sign and like-sign pairs in a single p+p and Au+Au collision where perfect electron identification is assumed. One can see the like-sign mass spectrum represents the combinatory background very well. The track quality cuts requires Nfit>20 and Nfit/Nmax> 0.5, where Nfit and Nmax are the number of fit points and maximum number of possible registered points for the reconstructed track .

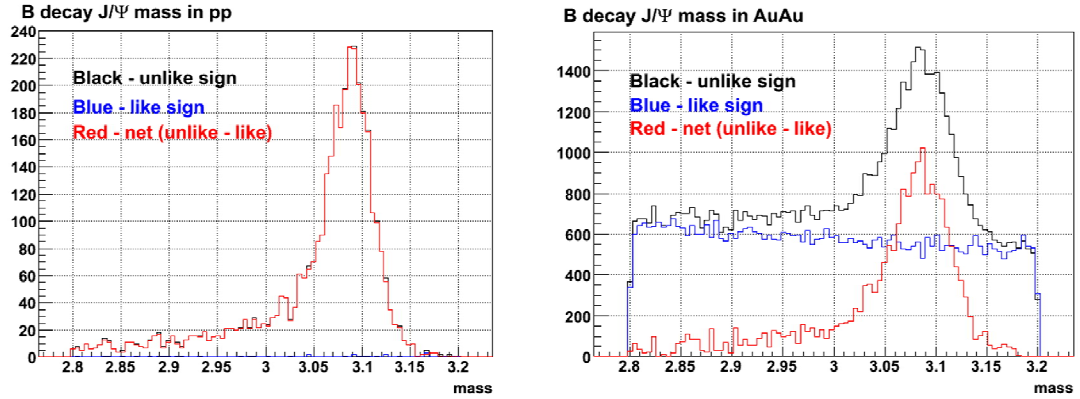

Figure 4: J/ψ mass distribution in single p+p collision and central Au+Au collisions. Black and blue histograms represent unlike, like-sign electron pairs, respectively; Red histogram is obtained after subtracting like-sign spectrum from unlike-sign spectrum. Note that 20 J/ψ–>ee are embedded into one Au+Au collision, therefore the S/B in the mass distribution does not reflect the actual value in real data.

Figure 5 shows the J/ψ pseudo-cτ distribution in most central Au+Au collisions where the left panel is for B→ J/ψ and the right panel is for direct J/ψ. The black and red histograms are the results from unlike-sign and like-sign pairs, respectively. The red histogram is obtained after subtracting the like-sign pairs from the unlike-sign pair distribution. If the technique works well, the like-sign pairs should represent the combinatory background and the red histogram should be the pseudo-cτ distribution for B-decay J/ψ. We

confirmed this by comparing the result with the one from tagged B-decay J/ψ which showed consistent results. Since direct J/ψ originates from the collision vertex, its pseudo-cτ distribution is expected to be a narrow Gaussian peak centering at zero with the width determined by the tracking resolution. In the Figure 5 one can see that beside the expected Gaussian peaks, there are additional tails on both positive and negative side that are most likely coming from the misassociation of reconstructed track and PIXEL hits. As we will show later, similar tails are seen in CDF measurements. The B-decay J/ψ distribution contains a long tail in the positive pseudo-cτ due to the long B meson life time, a sharp Gaussian tail on the negative region due to tracking resolution and a tail due to the misassociation of tracks and PIXEL hits as in the case of direct J/ψ.

Figure 6 shows the pseudo-cτ distribution for B-decay and direct J/ψ in most central Au+Au collisions with and without PIXEL pile-up effect. The normalization used the one in p+p collisions. The FONLL calculation [15] predicts the total $b\bar{b}$ cross section in p+p collisions at RHIC is 1.87μb which leads to 3.74 μb for B meson production. Measurements from PHENIX run2005 p+p collisions show that the total direct J/ψ→e^+e^- production is about 178nb. Taking into account the B→J/ψ→e^+e^- branching ratio, we obtained the yield ratio of direct J/ψ over B-decay J/ψ is about 65. The results show that the tail from the track and PIXEL hits misassociation is the major background for measuring B mesons. This background becomes larger when pile-up effect is added and it is demonstrated more clearly in the change of S/B ratio before and after adding the pile-up effect.

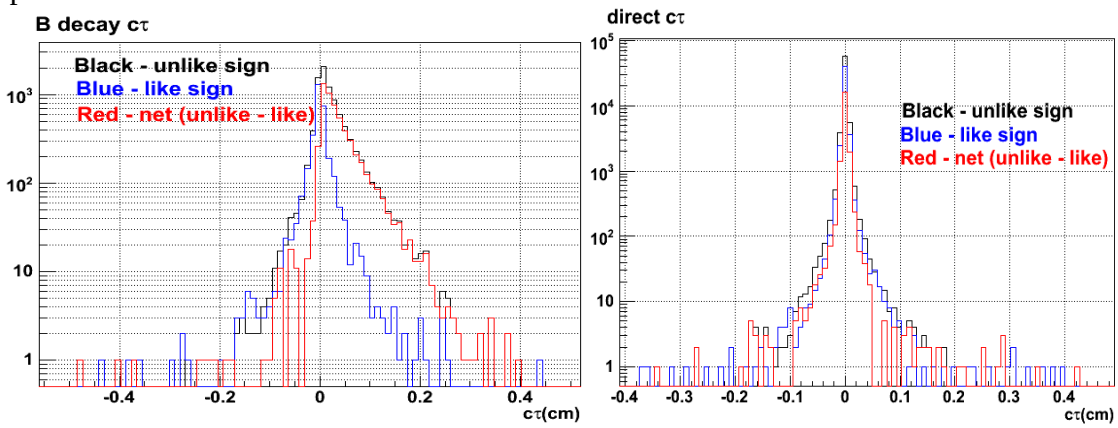

Figure 5: pseudo-ct distribution for the B-decay J/ψ (left panel) and direct J/ψ (right panel). See text for details.

Figure 7 shows the S/B ratio and efficiency in measuring B meson as a function of cut on pseudo-cτ. One can see that the effect from pile-up increase when the cut increase. This is because the pileup hits on PIXEL detector enhance the probability of track and PIXEL hits misassociation which is the source for the non-Gaussian tail in the pseudo-cτ distribution. The results shows that the S/B ratio reach maximum of 1~2 at a pseudo-cτ cut at 500μm where the efficiency for B-decay J/ψ is about 30%. Notice that these results do not include any nuclear or QGP effects for J/ψ and B meson production. As we know from the PHENIX run2004 measurement[18], J/ψ production at mid-rapidity suppressed by a factor of three in most central Au+Au collisions. If B meson is much less suppressed, the S/B ratio can increase significantly. In the real data analysis, one way to measure the B→J/ψ yield is to obtain, for example, the background p_T shape by applying

a very small pseudo-cτ cut. After that one apply a large cut to obtain the B-decay J/ψ p_T shape using the background shape as a reference.

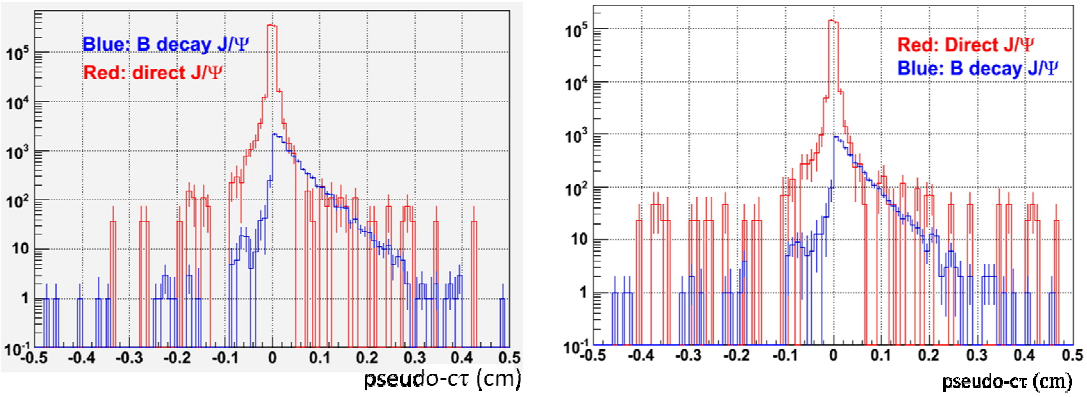

Figure 6: pseudo-cτ distribution for direct and B-decay J/ψ in more central Au+Au collisions before (left panel) and after (right panel) including PIXEL detector pile-up effect in 1× RHIC-II luminosity. The red and blue histograms are from direct and B-decay J/ψ, respectively.

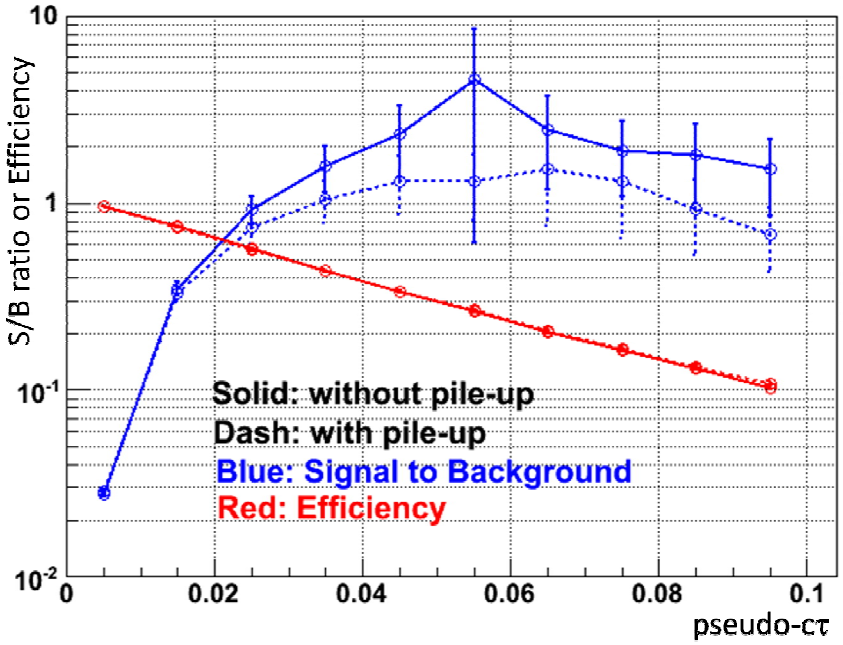

Figure 7: S/B ratio and efficiency as a function of pseudo-ct cut for B→J/ψ measurements in most central Au+Au collisions. The dashed curves represent result including PIXEL pile-up effect in 1× RHIC-II luminosity. The red curves are efficiency and blue curves are S/B ratio. The error bars are statistical errors only.

We then studied the effect of PIXEL detector position resolution on the measurements. Figure 8 present the results when PIXEL detector resolution is changed from 8μm to 80μm without including the pile-up effect. We changed the electron pair DCA cut from 50μm to 200μm to keep the efficiency unchanged. Left panel shows pseudo-cτ distribution for direct and B-decay J/ψ. Compared to the results in the left panel of Figure 6, one can see the distribution for direct J/ψ become much wider due to the worse resolution while the effect on B-decay J/ψ is not that obvious due to the much larger B meson cτ. The widened direct J/ψ distribution leads to five to ten times smaller S/B

which is shown in the right panel of the figure. Therefore HFT PIXEL detector is unique in this measurement.

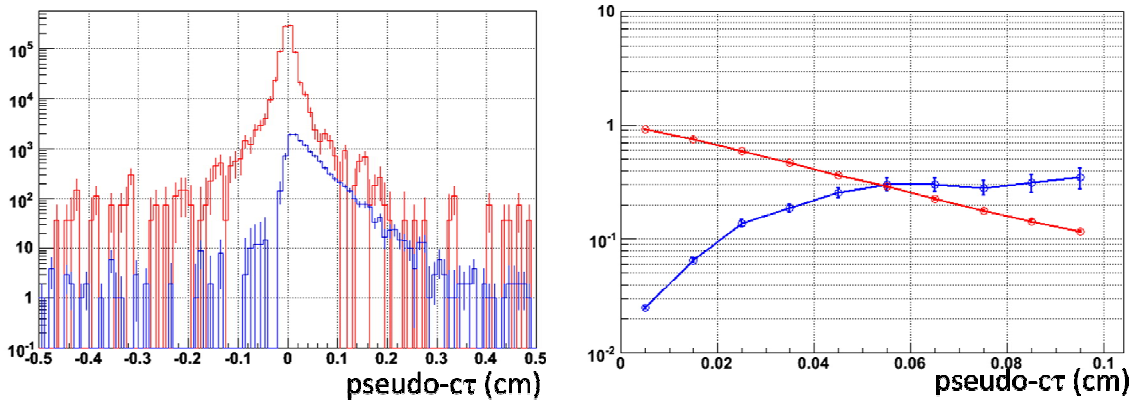

Figure 8: Results after changing the PIXEL detector position resolution from 8μm to 80μm; Left panel is pseudo-cτ distribution for direct J/ψ (red) and B-decay J/ψ (blue); right panel is the S/B (blue) and efficiency (red) as a function of pseudo-cτ cut.

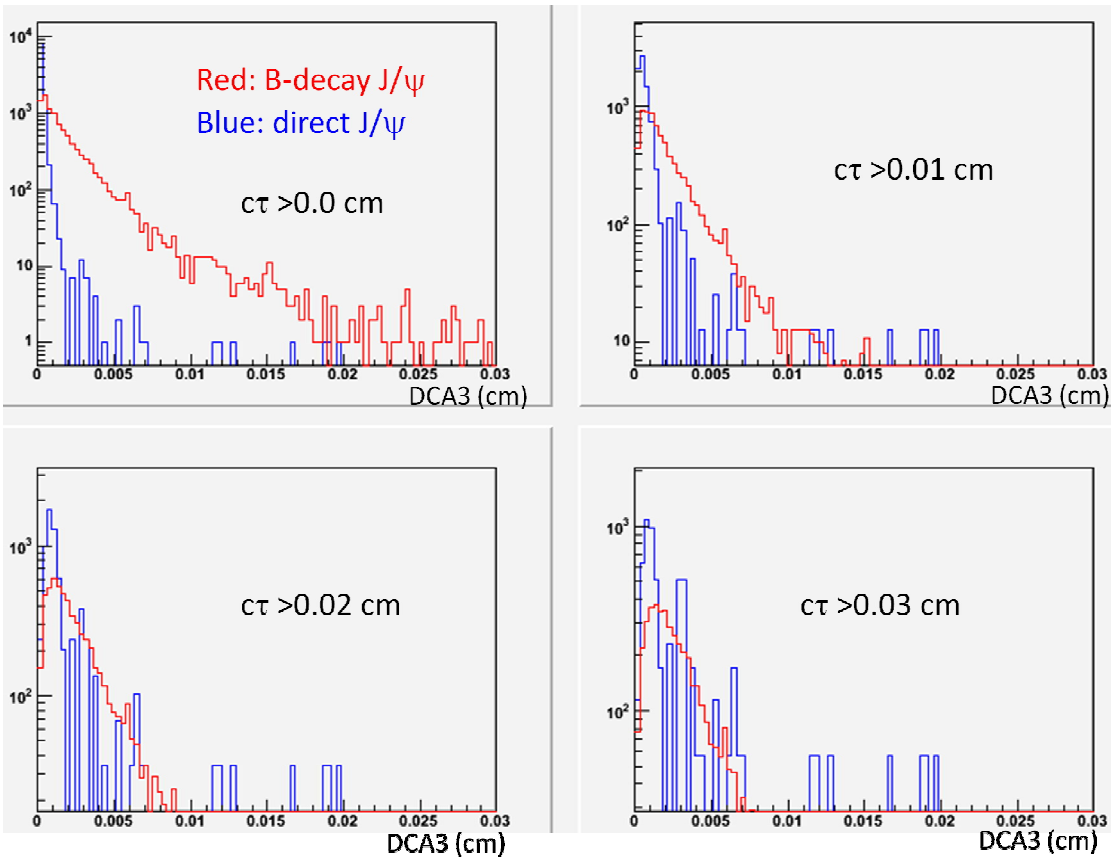

Figure 9: Distribution of the minimum distance of closest approach between a third charged particle to the reconstructed production point of J/ψ under different pseudo-cτ cut. Red histogram is for B-decay J/ψ and blue histogram is for direct J/ψ.

One possible way to improve the S/B is by applying the cut on the distance of closest approach on a third charged particle (DCA3) to the reconstructed J/ψ production point. A large fraction of 'X' particles from B→J/ψ+X are charged. In large cτ region, ideally

after applying a small DCA3 cut, namely DCA3<cut, most of the direct J/ψ which come from collision point were expected to be rejected while a large fraction of B-decay J/ψ should be kept. It turns out that the small DCA3 cut can't improve the S/B ratio. Figure 9 shows the DCA3 distribution under different pseudo-cτ cut. When no pseudo-ct cut is applied, the direct J/ψ DCA3 distribution is much narrower than the B-decay J/ψ since at collision vertex there are thousands of charged particles can be used as a third particle to reconstruct DCA3 and it is very likely for a randomly associated third particle to be closer than the reconstructed position of the actual third partner. When pseudo-cτ cut is larger, this probability become smaller and the distribution become wider. In large ct region, as shown in the figure, the results for direct and B-decay J/ψ become very similar, therefore cutting on DCA3 can't improve S/B ratio. However, based on Figure 9, applying a large DCA3 cut, for example DCA3>20μm will enhance the S/B especially when small pseudo-cτ cut is applied. Figure 10 shows the result after this cut without including the PIXEL detector RHIC-II pile-up effect. One can see that the DCA3 cut dramatically improved the S/B ratio in the small pseudo-cτ cut region but have little effect in the large pseudo-cτ cut region. In the mean time, the B-decay J/ψ suffers significant efficiency loss. Therefore, the analyses with and without DCA3 cut can be used to cross check each other to understand systematic uncertainties.

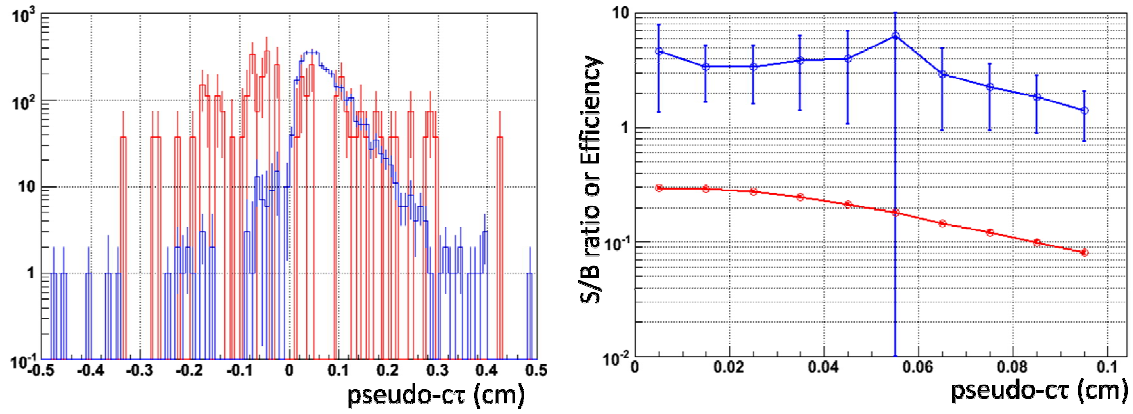

Figure 10: Results after applying the DCA3 cut; Left panel is pseudo-cτ distribution for direct J/ψ (red) and B-decay J/ψ (blue); right panel is the S/B (blue) and efficiency (red) as a function of pseudo-cτ cut

We also did a consistency check between our results and CDF measurements. Figure 11 shows CDF measurements on B→J/ψ. The left panel presents the breakdown of pseudo-cτ distribution for different components in RUN-I where only high p_T J/ψ (p_T>5GeV) are measured. One can see the shape for direct and B-decay J/ψ are similar to what we observed including the tail represented by an exponential curve due to the misassociation of track and their silicon detector hits. One can estimate from the figure that without including the "background", the S/B ratio is about 10 compared to ~2 at RHIC. The right panel shows that the relative yield of direct J/ψ over B-decay J/ψ is about 15 compared to 65 at RHIC. Assuming CDF detector and STAR detector have similar performance in measuring B→ J/ψ, these two results are consistent with each other. The "background" indicated in the figure comes from the continuum and Drell/Yan which is about 10% of direct J/ψ in terms of production yield judging from the figure. However, they produce comparable tails in large pseudo-cτ region to those from direct J/ψ. The inclusive p_T J/ψ measurements from PHENIX indicate a similar relative yield of charm continuum and

Drell/Yan over direct J/ψ. We therefore can expect they have similar level of contribution as direct J/ψ in the large pseudo-cτ region at RHIC.

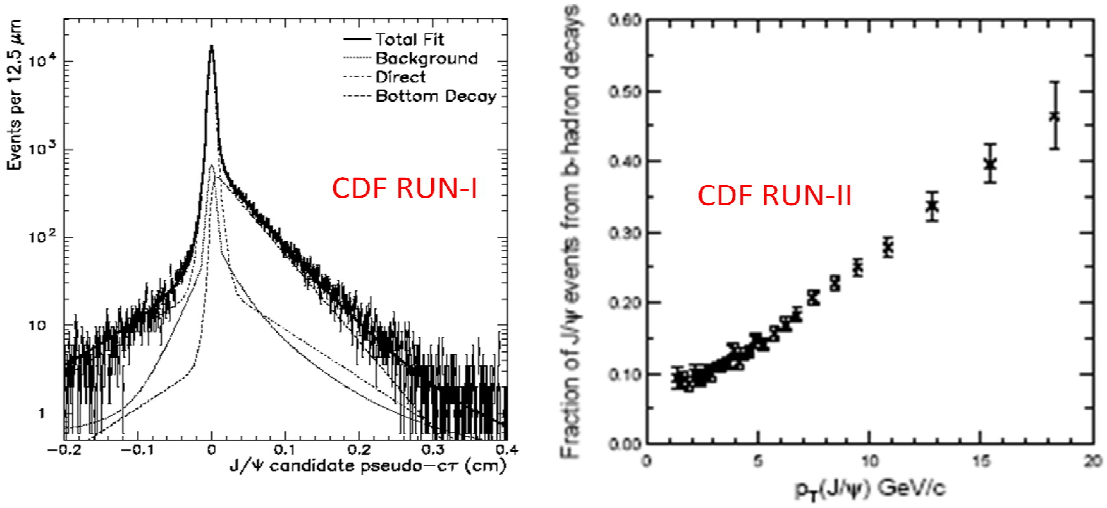

Figure 11: CDF measurements on B→J/ψ decay. Left panel shows the pseudo-cτ distribution in RUN-I with breakdown of different source of contribution; right panel shows the ratio of B-decay J/ψ over the direct J/ψ in RUN-II.

The number of B-decay J/ψ recorded in STAR during each RHIC-II week without including the trigger efficiency is:

$$N(B \to J/\psi) = \sigma(B) \cdot BR(B \to J/\psi) \cdot BR(J/\psi \to e^+e^-) \cdot AccpEff(recon) \cdot eff(p_T\ cut) \cdot eff(c\tau\ cut) \cdot eff(analysis\ cut) \cdot dutyFactor \cdot luminosity(RHIC - II)$$

, where $\sigma(B)$ is the B meson cross section; $BR(B \to J/\psi)\ and\ BR(J/\psi \to e^+e^-)$ are branching ratio for each of the decay channels; $AccpEff(recon)$ is the product of J/ψ acceptance and reconstruction efficiency in full phase space; $eff(p_T\ cut)$ is the efficiency due to the p_T >1.25GeV cut; $eff(c\tau\ cut)$ is the efficiency due to pseudo-cτ cut; $eff(analysis\ cut)$ is the efficiency for all the analysis cut including track quality, electron pair DCA and J/ψ mass window, etc; $dutyFactor$ is the expected STAR duty factor during the run; $luminosity(RHIC - II)$ is the expected delivered luminosity in a 12-week RHIC-II run in 2013[19]. The value for each of above variable is listed in the following table:

Variables	Single p+p collision	Au+Au collisions
$\sigma(B)$	3.7 μb	0.14b (assuming binary scaling)
$BR(B \to J/\psi)$	1.094%	1.094%
$BR(J/\psi \to e^+e^-)$	5.94%	5.94%
$AccpEff(recon)$ |collision Zvtx| <5cm	17.4% (direct J/ψ), 19.4% (B→J/ψ).	12.2% (direct J/ψ.)[a] 13.6% (B→J/ψ)[a]
$AccpEff(recon)$ without collision Zvtx cut .30 cm diamond Zvtx	3.1% (direct J/ψ) 3.5% (B→J/ψ)[b]	2.2% (direct J/ψ)[b] 2.5% (B→J/ψ)[b]

$eff(p_T\ cut)$	76.0%	76.0%
$eff(c\tau\ cut)$	30%	30%
$eff(analysis\ cut)$	59%	59%
$dutyFactor$	70%	70%
$luminosity\ (RHIC-II)$ Maximum per 12 weeks Minimum per 12 weeks	 $360pb^{-1}$ $46pb^{-1}$	 $19nb^{-1}$ $3.3nb^{-1}$

a: Loss of efficiency compared to that in a single p+p collision due to high multiplicity.
b:Only the efficiency for direct J/y is from the simulation. All the tagged number are derived from the relative ratio calculated in AccpEff(reco) with 5cm Z vertex cut.

The total number of $B\rightarrow J/\psi\rightarrow e^+e^-$ per RHIC-II 12-week run recorded at STAR *assuming 100% trigger efficiency* and neglecting TPC pile-up effect in high collision rates:

- In p+p collisions,
  - Maximum: 2858±93 J/ψ at $p_T \geq 1.25$GeV/c
  - Minimum: 365±33 J/ψ at $p_T \geq 1.25$GeV/c
- In Au+Au collisions
  - Maximum: 4066±110 J/ψ at $p_T \geq 1.25$GeV/c
  - Minimum: 706±46 J/ψ at $p_T \geq 1.25$GeV/c

Based on these numbers, we then calculated the number of J/ψ recorded at |Z vertex|<5cm by multiplying the efficiency (13.2%) of the vertex cut estimated from a Gaussian distribution with σ=30cm and *assuming 100% trigger efficiency:*.

- In p+p collisions
  - Maximum: 2084±79 J/ψ at $p_T \geq 1.25$GeV/c.
  - Minimum: 266±28 J/ψ at $p_T \geq 1.25$GeV/c.
- In Au+Au collisions
  - Maximum: 2926±94 J/ψ at $p_T \geq 1.25$GeV/c
  - Minimum: 508±39 J/ψ at $p_T \geq 1.25$GeV/c.

Therefore, about 70% of the observed J/ψ are from |Z vertex|<5cm due to the configuration of PIXEL detector.

However, the J/ψ trigger performance in STAR will have to be significantly improved to make it possible to measure $B\rightarrow J/\psi$. In p+p collision, the current J/ψ trigger efficiency based on the estimation from 2006 p+p run is only ~10% at $p_T(J/\psi)>6$GeV/c. If the trigger performance persist at RHIC-II, the maximum number of observed $B\rightarrow J/\psi\rightarrow ee$ per 12-week run is ~2858*10%*3% = 9, where 3% is the fraction of J/ψ at $p_T>6$GeV/c relative to the number of J/ψ at $p_T>1.25$GeV/c. This means $B\rightarrow J/\psi\rightarrow ee$ channel cannot be used to measure B meson without improved trigger. In Au+Au collision, the expected collision rate is ~50 kHz. Considering the 1 kHz, STAR DAQ bandwidth, we will also need a very good J/ψ trigger to carry on this measurement. With the TOF and DAQ1000 upgrade, the J/ψ trigger is expected to be significantly improved. New studies are needed to estimate the improvement. One the other hand, when the Muon Telescope Detector (MTD) upgrade is accomplished, we can study B meson using $B\rightarrow J/\psi\rightarrow \mu^+\mu^-$ channel

using high performance MTD trigger which is expected to have very high rejection power.

---

[1] Y. L. Dokshitzer *et al.*, Phys. Lett. **B 519**, 199 (2001).
[2] G. D. Moore, and D. Teaney, Phys. Rev. **C71,** 064904 (2005).
[3] H. van Hees *et al.*, Phy. Rev. **C 73,** 034913 (2006); (private communication)
[4] S. Wicks *et al.*, Nucl. Phys. **A 784**, 426 (2007).
[5] M. Djordjevic, nucl-th/07053439.
[6] A. Adil, and I. Vitev, Phys. Lett. **B 649**, 139 (2007)
[7] I. Vitev, A. Adil, and H. van Hees, Journal of Physics G-Nuclear and Particle Physics **34**, S769 (2007).
[8] X. Lin et al., STAR Coll., J. Phys G 34, S295 (2007); Gang Wang et al., STAR Coll., arXiv:0804.4448 [nucl-ex].
[9] Rosario Turrisi et al., ALICE Coll., ACTA PHYSICA POLONICA B38, 1039 (2007).
[10] C. Albajar et al., UA1 Coll., Phys. Lett. B213, 405 (1988); C. Albajar et al., UA1 Coll., Phys. Lett. B256, 121 (1991).
[11] D. Acosta et al., CDF Coll., Phys. Rev. D **71**, 092001 (2005)
[12] F. Abe et al., CDF Coll. Phys. Rev. D57, 9 (1998).
[13] C. Amsler *et al.*, Physics Letters **B667**, 1 (2008)
[14] C. Chasman et al., http://rnc.lbl.gov/hft/docs/hft_final_submission_version.pdf
[15] M. Cacciari et al., Phys. Rev. Lett. 95, 122001 (2005).
[16] B.I. Abelev et al., STAR Coll., Phys. Rev. Lett. 98, 192301 (2007).
[17] Rosario Turrisi et al., ALICE Coll., ACTA PHYSICA POLONICA B38, 1039 (2007).
[18] A. Adare et al., Phys. Rev. Lett. **98**, 232301 (2007)
[19] W. Fischer, T. Roser, et al., http://www.agsrhichome.bnl.gov/RHIC/Runs/RhicProjections.pdf